

Study of Wavefront Tilt Variance with Various Telescope Apertures in Indoor Convective Turbulence

Awakash Dixit^{#,*}, Aditya Kumar Mamgain[#], Vikash Porwal[#], and Sanjay Kumar Mishra^{#,*}

[#]*Adaptive Optics Division, DRDO-Instruments Research & Development Establishment, Dehradun - 248 008, India*

[@]*Uttarakhand Technical University, Dehradun - 248 007, India*

^{*}*E-mail: skmishra@irde.drdo.in*

ABSTRACT

Turbulent atmosphere produces random wavefront tilts in the propagating laser beam and the dynamics of turbulence largely depends on the receiving optics aperture size. In this paper, wavefront tilt variance is studied with various telescope aperture sizes in indoor convective turbulence. A simple experimental setup is described for simulating the near ground atmospheric turbulence by generating different strengths of convective turbulence in the laboratory. A laser beam is made to propagate through the turbulence subsequently induced wavefront tilt variances are experimentally measured and analysed statistically. The wavefront tilt variance is used to estimate the temporal characteristics using Fourier transform by varying aperture sizes and turbulence strengths (i.e. ambient, weak and moderate). The Hurst exponent, the Fried parameter and the wavefront tilt frequencies for the different turbulence strengths are calculated. The power dependence of the wavefront tilt variance on the telescope aperture size is studied and a deviation from the classical $D^{-1/3}$ dependence is reported.

Keywords: Adaptive optics; Wavefront tilt variance; Convective turbulence; Hurst exponent, Fried parameter; Non-Kolmogorov turbulence

1. INTRODUCTION

Atmospheric turbulence gives rise to random phase and amplitude fluctuations in an optical beam while propagating through the atmosphere. Adaptive optics (AO) is a technique which measures and compensates these phase fluctuations induced due to atmospheric turbulence¹. Adaptive optics is being used in a variety of applications as in astronomy², medical science (ophthalmology)³, laser beam shaping⁴, and microscopy⁵. One of the applications of AO is in the terrestrial imaging⁶, in which near ground horizontal propagation of optical beam takes place. The near-ground propagation is significantly different in terms of severe variations in turbulence in comparison to the vertical propagation that is more common in astronomy. In defence applications, Nd:YAG laser is very commonly used and if we consider, e.g., propagation of 100 mJ Nd: YAG laser pulse (say pulse width 10 ns) will not distort within the pulse, however pulse stretching may take place. Depending upon the duty cycle variations in position and focusing of pulses will be observed. The corresponding peak power 10 MW may also lead to thermal blooming effect. A near-ground horizontal propagation and the estimation of the receiver size are of primary concern in defence application, which led us to study the turbulence effects by varying the turbulence strengths and the aperture sizes.

Evidently, the wavefront tilt variance is a function of telescope aperture. Turbulence induced wavefront tilt variance

has extensively been studied theoretically for understanding its dependence on aperture size of the telescope. Bufton and Genatt⁷ agree with the $D^{-1/3}$ law in stellar observations. However, theoretically predicted Kolmogorov turbulence is hardly experienced in case of near-ground horizontal beam propagation. Significant experimental deviations have been reported^{8,9}. Further, for near ground horizontal propagation, the deviations have been experimentally confirmed in the case of indoor convective turbulence¹⁰. We have also observed the deviation from the classical $D^{-1/3}$ dependence. So far the experiments have been conducted for shorter path length and for small aperture sizes. We have extended the study to moderate size telescope apertures and for longer propagation path. In addition, the effect of telescope aperture size on the temporal spectra of the turbulence induced wavefront tilt is also studied.

Turbulent atmosphere produces time variant phase fluctuations in the laser beam while propagation. Various methods have been adopted to study the temporal spectra of phase-related quantities¹¹⁻¹³. These include measurement of some relevant parameters such as angle-of arrival (AOA) fluctuations using image centroid motion^{11,12} and variances of piston and tilt motions of the mirror segments of the corrector¹³. The temporal behaviour of turbulence has been extensively studied theoretically¹⁴⁻¹⁵. This has been employed to determine the bandwidth of an adaptive optics system¹¹. Such temporal frequency power spectra have been determined by tilt data (using Zernike expansion coefficients) for a point

source with Kolmogorov turbulence¹⁵ and other approaches, viz., fringe motion, image motion differential AOA, etc¹⁶. Most of these studies are for stellar observations involving vertical turbulence path and fixed aperture sizes. Determination of wavefront tilt frequency is an important parameter for deciding the closed-loop servo bandwidth of an Adaptive optics imaging system. To the best of our knowledge, no attempt has so far been made to study the aperture dependency of the variance of wavefront tilt and the frequency spectra in the case of near ground turbulence with horizontal propagation. We have carried out the temporal frequency analysis of turbulence induced wavefront tilt with different aperture sizes.

In the near ground atmosphere, the thermal effects is mainly attributed to free convection phenomenon. Due to differential solar heating of the ground and re-radiation of the long wave terrestrial radiations, convective air currents are generated in the atmospheric layers adjacent to the ground. The phenomenon is most accentuated within the surface layer extending upto 50 m - 300 m, depending on the location. At higher altitudes, however, horizontal wind flow pre-dominates the convection phenomenon and Kolmogorov statistics can be applied satisfactorily¹⁷.

Usually, atmospheric turbulence can be generated in the laboratory by the three methods:

- (i) rotating static phase screens
- (ii) dynamic reconfigurable phase screens and
- (iii) turbulent fluid chambers⁹.

Atmospheric turbulence has been generated by the two methods in the laboratory for small beam sizes:

- (i) phase plate (based on Near-Index-Matched method with a motorised assembly) which has low dynamics limited by the speed of the stepper motor¹⁸ and
- (ii) hot-air chamber, which has high dynamics¹⁹.

Thermally induced turbulence has been reported as being representative of the near-ground atmospheric turbulence²⁰. To simulate the near ground turbulence, we generated thermal convective currents employing a set of electric heaters and pedestal fans.

In this paper, wavefront tilt variances induced by indoor convective turbulence are measured and analysed statistically. The turbulence strength and the tilt frequency spectra are estimated from the mean variance of the spot motion by varying the aperture sizes and turbulence strengths. A trend in the variation of weights of tilt frequencies with different aperture sizes is observed, however, any empirical relationship is not established. The Hurst exponent (H) and Fried parameter (r_0) for different turbulence cases are also calculated.

2. MATHEMATICAL FORMULATION

A generalised model describing wavefront tilt variance for near ground non-Kolmogorov turbulence is adopted, which is more suitable²¹.

$$\sigma_H^2 = \frac{\Gamma(2H+1)\Gamma(H+1/2)\Gamma(1-H)\sin\pi H}{\pi^{3/2}2^{(2H-3)}\Gamma(H+1)\Gamma(H+2)} \times \frac{C_\phi^2}{2\pi^2} \lambda^2 r_0^{-2H} D^{2H-2} \quad (1)$$

where σ_H^2 is the generalised wavefront tilt variance, C_ϕ^2 is the phase structure constant ($C_\phi^2 = 6.88$) and H is the power

exponent. Based on above model, the power dependence of wavefront tilt variance is estimated on telescope aperture size. The power exponent H , commonly known as Hurst exponent²², has a bounded range between 0 and 1. For the near ground experimental measurements, it has been reported that the Hurst exponent varies in the range (1/2, 5/6)⁸⁻⁹. This holds good for horizontal propagation in near ground turbulence and also for laboratory generated convective turbulence. For Kolmogorov turbulence ($H = 5/6$), the expression for variance reduces to the classical expression as propounded by Tatararski for two-axis wavefront tilt variance¹.

$$\sigma^2 \approx (6.88/2\pi^2)\lambda^2 r_0^{-5/3} D^{-1/3} \quad (2)$$

where D is the diameter of the circular aperture, λ is the wavelength and r_0 is the Fried parameter. The Fried parameter (r_0) is defined as the maximum diameter of receiving optics that is allowed before atmospheric distortion seriously limits the performance. The Fried parameter is widely used as a representative of the strength of turbulence integrated along the propagation path for a particular site and is the main parameter for designing an AO system. The values may vary from a few millimeters to a meter¹. For near ground horizontal propagation, its values lie in the range of a few tens of millimeters²⁰. For a horizontal path length, the Fried parameter (r_0) for plane waves is given¹ by Eqn. (3):

$$r_0 = 1.68(C_n^2 L k^2)^{-3/5} \quad (3)$$

where C_n^2 is the refractive index structure constant, L is the propagation path length, and k is the wave number. The refractive index structure constant is used to describe the atmospheric turbulence profile with altitude. Generally, the value of C_n^2 near the ground in warm climate¹ varies between 10^{-14} and $10^{-12} m^{-2/3}$. Once Fried parameter is measured, C_n^2 can also be estimated under the approximation of horizontal propagation using Eqn. (3).

3. EXPERIMENTAL SETUP

The experiment was performed in the laboratory over a range of 12 m. The experimental schematic is as shown in Fig. 1. The key components of the experimental set up are Schmidt-Cassegrain telescope (Meade LX-200 ACF), Optical beam positioner (Newport OPB U-96, Series L3130) for recording the laser spot motion, He-Ne laser with necessary optics, electric heaters and computer. A spatially filtered laser beam (He-Ne laser, $\lambda = 632.8$ nm, power 9.0 mW) was expanded with a Plano-convex lens ($f = 76.5$ mm) and propagated over the above said range. The atmospheric turbulence was simulated

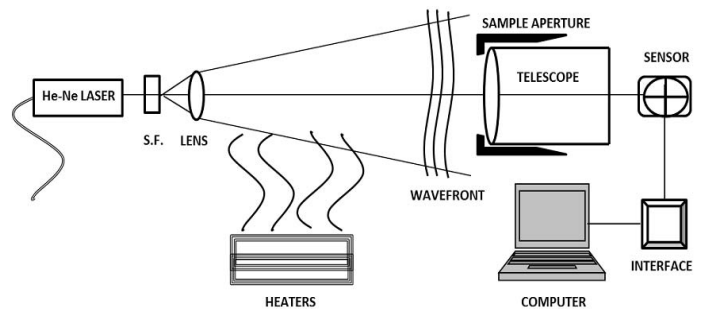


Figure 1. Experimental schematic.

by generating convective turbulence by using two electric heaters each of 1000 W of power and a fan (maximum rotation speed: 1200 rpm).

The optical waves propagated about 1m above the heaters and were collected using a Schmidt-Cassegrain telescope of aperture size 203.2 mm (diameter) and focal length 2000 mm. The telescope was set to infinity. The tilt introduced in the wavefront due to convective turbulence results in the spot motion at the focal plane of the telescope. To measure the spot motion, an optical beam positioner was placed at the telescope focus. The reference laser source and the telescope were both placed on the vibration isolation tables, so as to avoid the ambient mechanical vibrations.

4. RESULTS AND DISCUSSION

In the study, three different degrees of turbulence by switching on the heaters were generated and analysed. The characterising temperatures were measured with a mercury thermometer placed along the laser propagation axis that was about 1 m above the heaters. The generated turbulences were categorised into three cases with the respective measured temperatures (T) listed as follows:

- (a) Ambient $\langle T \rangle \sim 21.3^\circ\text{C}$
- (b) Weak turbulence $\langle T \rangle \sim 24.6^\circ\text{C}$
- (c) Moderate turbulence $\langle T \rangle \sim 27.2^\circ\text{C}$

For each case, the turbulence settling time was fixed for 30 min to obtain steady turbulence profile. The present scheme offers a good approximation to near-ground turbulence, which is convective in nature. To select different turbulence scales, circular apertures of six different sizes (diameter) viz. 90 mm, 115 mm, 140 mm, 165 mm, 190 mm and 203.2 mm are placed in front of the telescope. By changing the diameter of the receiving aperture, we select the different turbulent scales, i.e., different eddies contributing to the wavefront tilt. In similar experiments, the inner scale has been reported to be of the order of a few millimeters²⁴ while the outer scale was about a hundred millimeters²⁵. Thus it can be assumed that all our aperture sizes are in inertial range.

The optical beam position sensor measured the instantaneous x-y coordinates of the centroid of the spot. The data were captured at an acquisition rate of 500 Hz. Each data set was recorded for 4 s. We captured 10 such data sets (each containing 2000 sample data) for each of the six aperture sizes in the three turbulence strength cases. The typical laser spot motion is as shown in Figs. 2(a) - 2(b). The instantaneous position coordinates were employed to calculate the variance of the laser spot along the x and y-axis. The variance along the two axes was then analysed.

4.1 Frequency Spectra of Wavefront Tilt Variance

The data were analysed using the Digital Fourier Transform (DFT) in MATLAB platform. We calculated the Fourier spectrum of all the ten records, each containing 2000 data sets, for all the six aperture sizes in all the three turbulence strength cases. The average of these 10 Fourier spectra was then taken as being representative of a particular aperture size in a given turbulence strength case. Different tilt frequencies

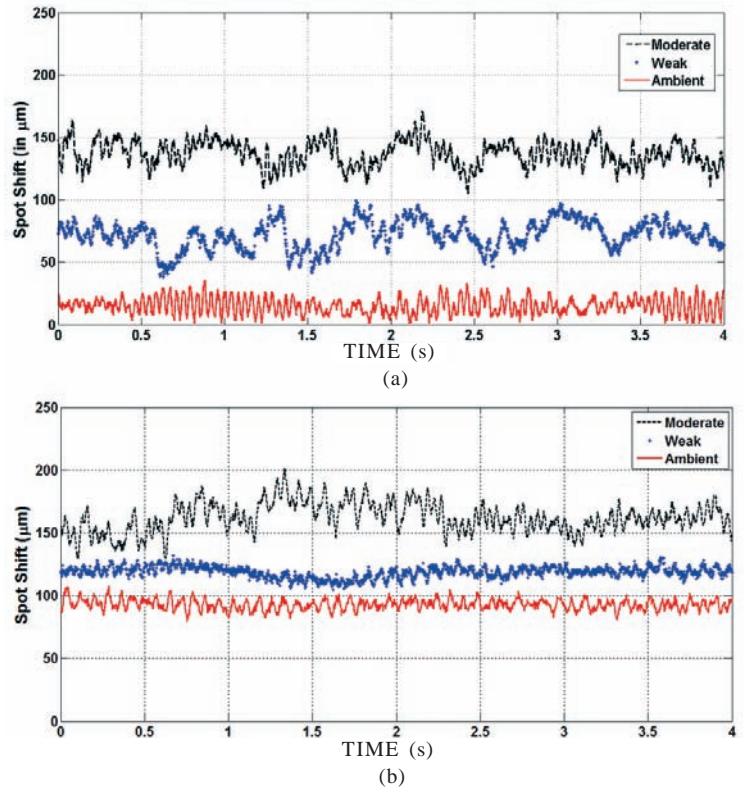
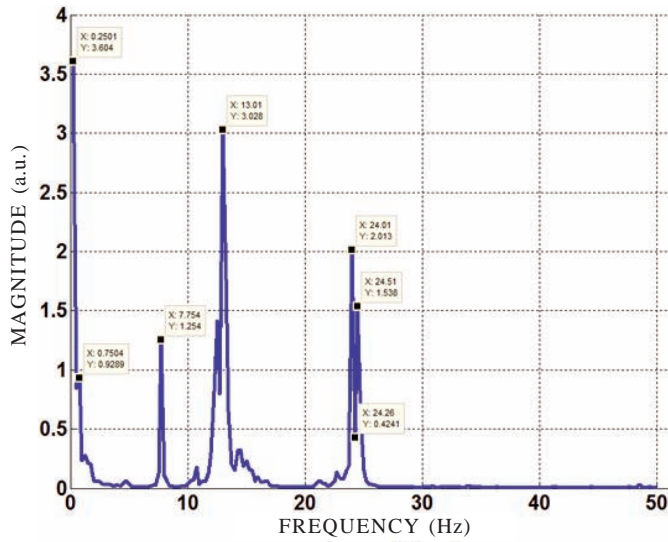


Figure 2. Laser spot motion in various turbulence conditions for (a) 90 mm and (b) 203.2 mm aperture diameter.

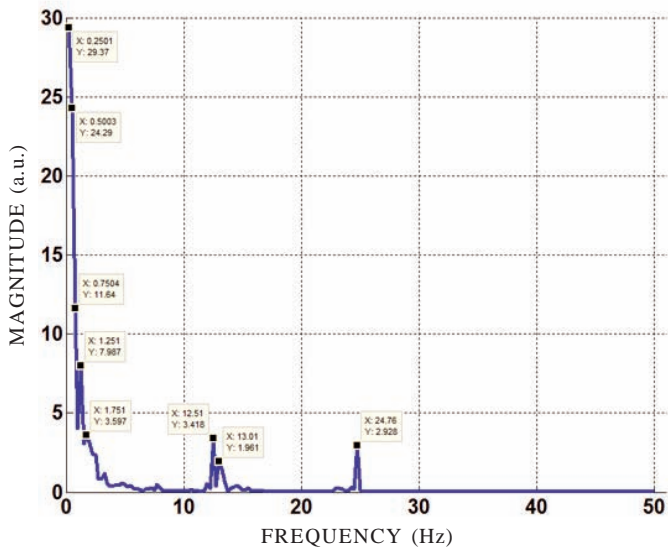
were found to be dominant at different turbulence scales corresponding to different aperture sizes. Figure 3(a) - 3(c) represent Fourier spectra for 203.2 mm aperture size for all the three turbulence strength cases. Similarly, Fourier spectra were calculated for data corresponding to other aperture sizes for all the three turbulence strength cases. We took into account only those tilt frequencies whose weight was found to be at least 10 per cent of the weight of the most dominant frequency. Applying this threshold criterion helped us to determine and select the significant frequencies as against the background noise. The tilt frequencies observed as common in all the cases were 1 Hz, 2 Hz, 3 Hz, 4 Hz, 8 Hz, 13 Hz, and 25 Hz (all rounded off to the nearest integer for simplicity). Lower frequencies (viz. upto 1 Hz or so) may be due to the platform or building vibrations and are not important for tilt frequency measurements. Though the experimental setup was placed on a stable platform, the possibility of platform vibrations could not be ruled out.

The effect of increasing turbulence strength on frequency content was also studied for commonly observed frequencies. While keeping the aperture size fixed, the weights of frequencies were plotted against the tilt frequencies for different turbulence strengths. In this manner the effect of various turbulence strengths was compared. The typical graph for the 90 mm aperture size is as shown in Fig. 4. A similar trend is also observed for other aperture sizes. It is evident from the analysis that the weight of all the tilt frequencies increases with increasing turbulence strength thereby showing the expected behaviour within experimental errors/limitations.

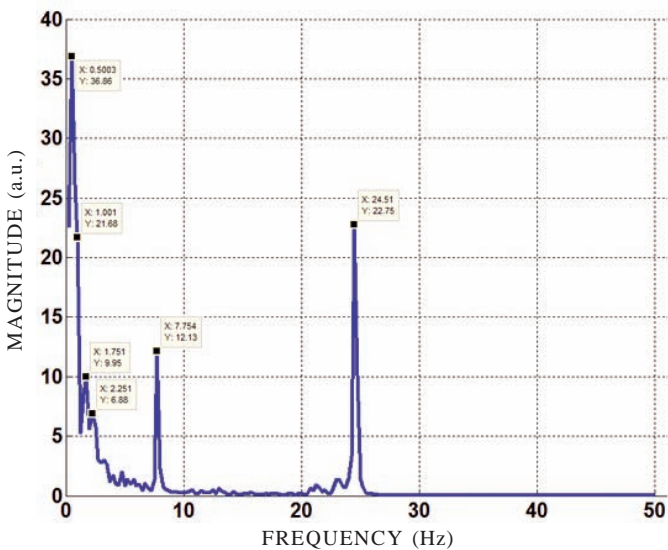
We further analysed the effect of the change in aperture size on the weight of tilt frequencies while keeping the turbulence



(a)



(b)



(c)

Figure 3. Frequency power spectrum for 203.2 mm aperture size (a) ambient, (b) weak turbulence, and (c) moderate turbulence.

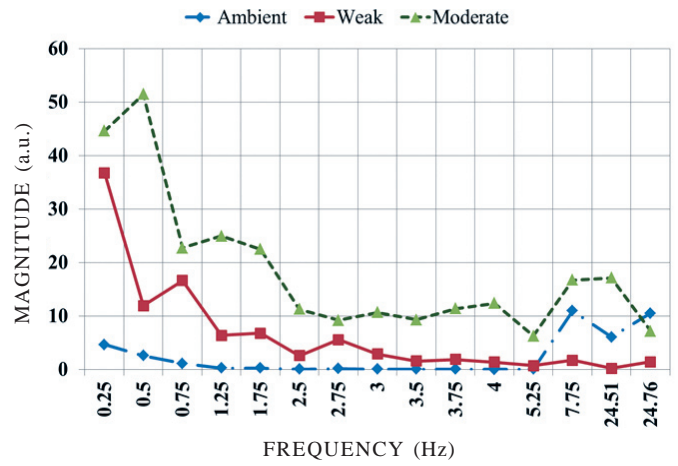


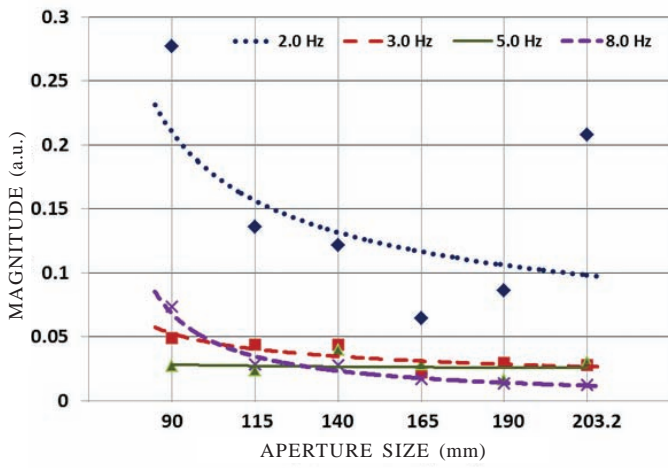
Figure 4. Comparison of frequencies content at different turbulence strengths for the aperture size of 90 mm.

strength fixed. Again we selected and compared those tilt frequencies which were observed for all the six aperture sizes. This was done for all the three turbulence strengths, i.e., ambient, weak and moderate. We adopted best power fit method for studying the variation of frequencies' weight with aperture size. Figures 5 (a) - 5(c) represents the weight of wavefront tilt frequencies as a function of aperture size. It is found that the weight of tilt frequencies decreases with increasing aperture size thereby indicating that in a given turbulence scenario the content of tilt frequencies tends to decrease at higher turbulence scales (i.e. larger aperture size). Thus it is clear that higher turbulence scales make lesser contributions to tilt frequencies. It appears from Figs. 5(a) - 5(c), that the power spectrum curves become less steep at higher turbulence strengths. That is, the weight of tilt frequencies falls off with increasing aperture size, more rapidly compared to the weaker turbulence strengths. Moreover, the weight of all the tilt frequencies appears to attain limiting values with increasing aperture size. Beyond a certain aperture size, the weight of these temporal frequencies should be independent of the aperture size as long as the aperture size remains below the outer scale. This can be verified by extending the experiment for even larger aperture sizes. Once the aperture size exceeds the outer scale (or reduced below the inner scale) phase damping effect may set into the picture and other effects may be expected. However, we did not investigate into this region because of the limited size of our telescope aperture. More data and larger aperture range together with controlled turbulence strengths are required to be studied in detail.

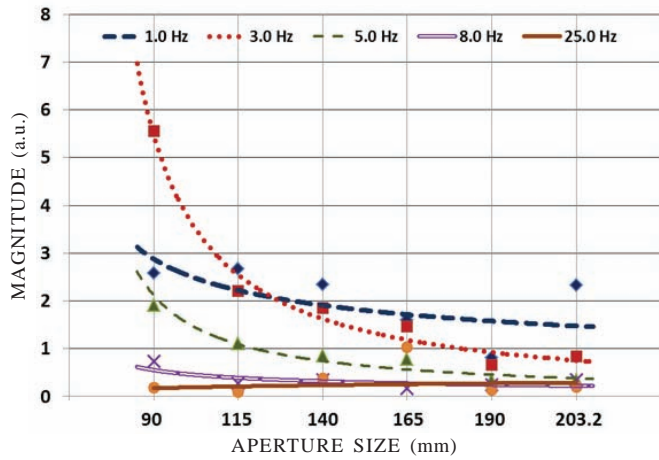
Thus, the dynamics of wavefront tilt for the near-ground turbulence with various apertures and turbulence strengths were studied. In all three cases of turbulence strength, the tilt frequencies were found to be limited to 25 Hz for all the receiving aperture sizes.

4.2 Wavefront Tilt Variance Study with Aperture Size

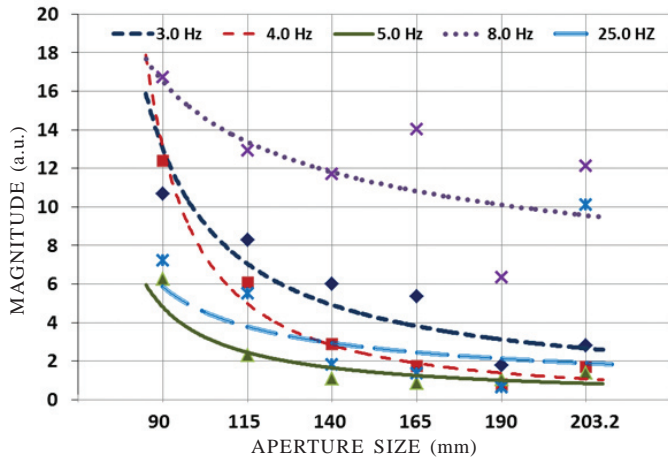
The variances corresponding to the radial shifts of spot centroid motion were calculated for each sample. The mean variance was then estimated by averaging the variances of the 10 samples for each aperture size. The process was repeated



(a)



(b)

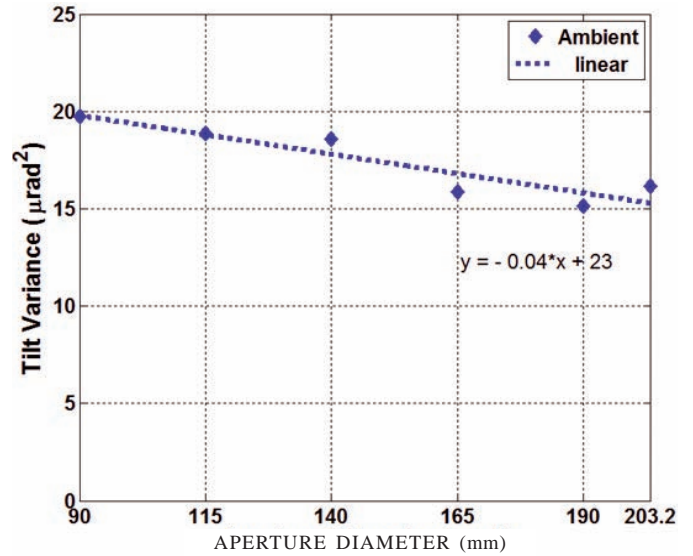


(c)

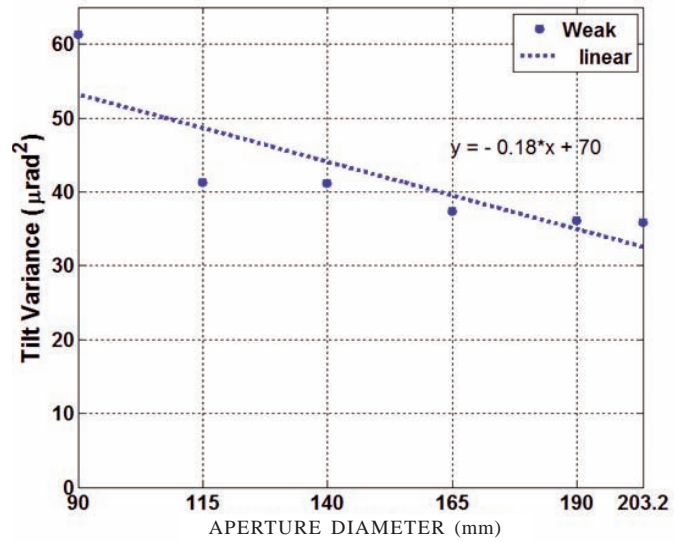
Figure 5. Variation in different frequencies weight with various aperture sizes (a) Ambient turbulence, (b) Weak turbulence, and (c) Moderate turbulence.

for all the three turbulence strengths. Figures 6(a) - 6(c) shows the estimated variances as a function of aperture diameter for the three turbulence strengths.

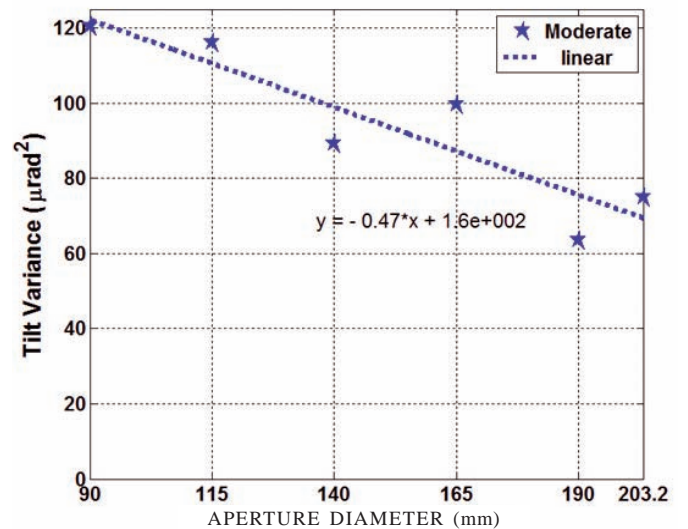
As shown in Figs. 6(a) - 6(c), the variance of the radial shifts of the focal spot decreases with increase in aperture size. With the help of best-fit method, the rate of change of variance (or slope) was determined. The absolute slopes estimated for



(a)



(b)



(c)

Figure 6. Variation in wavefront tilt variance for different turbulence strengths (a) Ambient turbulence, (b) Weak turbulence, and (c) Moderate turbulence.

ambient, weak and moderate turbulences were - 0.04, - 0.18 and - 0.47, respectively. The slope was found to increase with the increasing strength of turbulence thereby indicating that with increasing turbulence strength the wavefront tilt variance falls off more rapidly with increasing aperture sizes.

4.3 Estimation of Hurst Exponent and Fried Parameter

The Hurst exponent (H) is calculated by applying slope fit method on the tilt variance data for the different turbulence scenario. Using the calculated values of H , we estimated the Fried parameter (r_0) using Eqn. (1). Generally, r_0 is estimated using the Eqn. (2) that represents Kolmogorov approximated turbulence. In the case of near horizontal ground propagation, the use of Kolmogorov approximated r_0 estimation shows significant error. Results are as given in Table 1. The estimated values of Fried parameter are found in good agreement with the actually observed values for near ground turbulence conditions^{23,26}. The experimentally measured values of the Hurst exponent (H) show a departure from the classical $D^{-1/3}$ relation. In our experiment, the power dependence of aperture follows $D^{-0.04}$, $D^{-0.18}$, and $D^{-0.47}$ for ambient, weak and moderate turbulences, respectively. Hence, the generated convective turbulence follows non-Kolmogorov statistics thereby signifying the observed behaviour of near ground turbulence.

Table 1. Experimentally measured values of H and r_0

Turbulence strength	H	r_0 (mm)	
		Non-kolmogorov	Kolmogorov
Ambient	0.98	91.7	80.5
Weak	0.91	56.2	50.2
Moderate	0.76	27.8	30.5

From the results obtained in the experiment, it is observed that there were no sudden falls in wavefront tilt variance for small and large apertures, i.e., phase damping effects are not observed. As inner and outer scales are independent of turbulence flow, we can safely assume that all our aperture sizes are within inertial range. It must be stressed here that all the observations presented are based on two premises. First, all aperture sizes are in inertial range and second, the turbulence is isotropic. We have ignored the central obstruction of the telescope aperture. The effects of an annular aperture may be more than that obtained by just blocking the contributions from those turbulence scales which are smaller than the obstruction. The optical alignment of the apertures with the telescope axis was done manually. Although extreme care has been taken to ensure proper alignment, any misalignment would result in erroneous measurements.

5. CONCLUSIONS

In this paper, a simple experimental setup is described for generating various strengths of near ground convective turbulence in the laboratory. Wavefront tilt variances were measured and analysed statistically. As the study of tilt variance in the presence of indoor convective turbulence has been largely

confined to very small size apertures and shorter path lengths, we extended the study to moderate size telescope apertures and for longer propagation path. A precise procedure for estimating the Fried parameter and the wavefront tilt frequency has been established. These two parameters are used in designing an adaptive optics (AO) system. The wavefront tilt frequencies are used for determining the closed-loop servo bandwidth of a typical AO system. The wavefront tilt frequencies are observed to be limited to 25 Hz. The wavefront tilt variance decreases with increasing aperture sizes for all the three cases of turbulence. Therefore, it is concluded that larger aperture sizes make the lesser contribution to the wavefront tilt. The Fried parameter is estimated by applying Non-Kolmogorov and Kolmogorov statistics models for different turbulence cases. In the case of ambient and weak turbulence, the use of Kolmogorov model in estimating r_0 leads to lower values, whereas in the case of moderate turbulence it overestimates. Therefore, for designing an AO system for moderate turbulence, a procedure is presented in the paper for accurate estimation of the turbulence parameters in near ground turbulence scenarios.

REFERENCES

1. Tyson, R.K. Principle of adaptive optics. Edn. 3rd, CRC press, Boca Raton, 2011.
2. Scharmer, G.B.; Dettori, P.M.; Lofdahl, M.G. & Shand, M. Adaptive optics system for the new Swedish solar telescope. *In Proceedings of Astronomical Telescopes and Instrumentation SPIE*, 2003, 370-380. doi: 10.1117/12.460387
3. Hammer, D.X.; Ferguson, R.D.; Bigelow, C.E.; Ifimia, N.V.; Ustun, T. E. & Burns, S.A. Adaptive optics scanning laser ophthalmoscope for stabilized retinal imaging. *Opt. Exp*, 2006, **14**(8), 3354-3367. doi: 10.1364/OE.14.003354
4. Samarkin, V. & Kudryashov, A. Deformable mirrors for laser beam shaping. *In Proceedings Optical Engineering+Applications SPIE*, 2010, 77890B. doi: 10.1117/12.863965
5. Sherman, L.; Ye, J.Y.; Albert, O. & Norris, T. B. Adaptive correction of depth-induced aberrations in multiphoton scanning microscopy using a deformable mirror. *Journal Microscopy*, 2002, **206**(1), 65-71. doi: 10.1046/j.1365-2818.2002.01004.x
6. Levine, B.M.; Martinsen, E.A.; Wirth, A.; Jankevics, A.; Toledo-Quinones, M.; Landers, F.M. & Bruno, T. L. Horizontal line-of-sight turbulence over near-ground paths and implications for adaptive optics corrections in laser communications. *In Proceedings Optical Science Engineering and Instrumentation SPIE*, 1997, 354-365. doi: 10.1117/12.283899
7. Buffon, J. & Genatt, S.H. Simultaneous observations of atmospheric turbulence effects on stellar irradiance and phase. *Astronomy J.*, 1971, **76**, 378-386.
8. Masciadri, E. & Vernin, J. Optical technique for inner-scale measurement: possible astronomical applications. *Appl. Opt.*, 1997, **36**(6), 1320-1327. doi: 10.1364/AO.36.001320
9. Keskin, O.; Jolissaint, L. & Bradley, C. Hot-air optical turbulence generator for the testing of adaptive optics

- systems: principles and characterization. *Appl. Opt.*, 2006, **45**(20), 4888-4897. doi: 10.1364/AO.45.004888
10. Gulich, D.; Funes, G.; Zunino, L.; Pérez, D.G. & Garavaglia, M. Angle-of-arrival variance's dependence on the aperture size for indoor convective turbulence. *Opt. Comm.*, 2007, **277**(2) 241-246. doi: 10.1016/j.optcom.2007.05.018
 11. Soules, D.B.; Drexler, J.J.; Waldie, A.H.; Qualtrough, J.A.; Eaton, F.D.; Peterson, W. A. & Hines, J. R. Temporal characteristics of turbulence-induced image motion. *In Proceedings Propagation Engineering SPIE*, 1989, 224-33. doi: 10.1117/12.960875
 12. Martin, H. M. Image motion as measure of seeing quality. *Publications of the Astronomical Society of the Pacific*, 1987, 1360-1370.
 13. Greenwood, D.P. & Fried, D.L. Power spectra requirements for wave-front-compensative systems. *J.O.S.A.*, 1976, **66**(3), 193-206. doi: 10.1364/JOSA.66.000193
 14. Greenwood, D.P. Bandwidth specification for adaptive optics systems. *J. O. S. A.*, 1977, **67**(3), 390-393. doi: 10.1364/JOSA.67.000390
 15. Hogge, C. & Butts, R. Frequency spectra for the geometric representation of wavefront distortions due to atmospheric turbulence. *IEEE Trans. Antennas Propag.*, 1976, **24**(2), 144-154. doi: 10.1109/TAP.1976.1141310
 16. Conan, J.M.; Rousset, G.P. & Madec, Y. Wave-front temporal spectra in high-resolution imaging through turbulence. *J.O.S.A. A*, 1995, **12**(7) 1559-1570. doi: 10.1364/JOSAA.12.001559
 17. Jacobson, M.Z. Fundamentals of atmospheric modeling. Edn. 2nd., Cambridge University Press, New York, 2005.
 18. Mishra, S.K.; Dixit, A.; Porwal V. & Mohan, D. Design and testing of customized phase plate as atmospheric turbulence simulator. *In Proceedings of XXXVII National Symposium of OSI*, 2013, 172. doi: 10.13140/2.1.4106.5920.
 19. Dixit, A.; Porwal, V.; Mishra, S.K.; Kumar A.; & Gupta, A. K. Characterization of atmosphere-like turbulence for the performance evaluation of adaptive optics system. *In Proceedings of International Conference on Optics and Photonics*, 2015, 72. doi: 10.13140/2.1.4493.6489.
 20. Consortini, A. & O'Donnell, K.A. Measuring the inner scale of atmospheric turbulence by correlation of lateral displacement of thin parallel laser beam. *Waves Random Media*, 1993, **3**(2), 85-92. doi: 10.1088/0959-7174/3/2/003
 21. Pérez, D.G.; Zunino, L. & Garavaglia, M. Modeling turbulent wave-front phase as a fractional Brownian motion: a new approach. *J.O.S.A. A*, 2004, **21**(10), 1962-69. doi: 10.1364/JOSAA.21.001962
 22. Feder, J. Fractals. Plenum Press, New York, 1988.
 23. Razdan, A.K. Measurement of atmospheric turbulence parameters relevant to adaptive optic system design. *In Proceedings High-Power Lasers and Applications SPIE*, 2003, 124-131. doi: 10.1117/12.479215
 24. Consortini, A.; Sun, Y.Y.; Innocenti, C. & Li, Z.P. Measuring inner scale of atmospheric turbulence by angle of arrival and scintillation. *Opt. Comm.*, 2003, **216**(1), 19-23. doi: 10.1016/S0030-4018(02)02294-0
 25. Consortini, A.; Innocenti, C. & Paoli, G. Estimate method for outer scale of atmospheric turbulence. *Opt Comm*, 2002, **214**(1), 9-14. doi: 10.1016/S0030-4018(02)02117-X
 26. Cole, W.P. & Marciniak, M.A. Path-averaged C_n^2 estimation using a laser-and-corner-cube system. *Appl. Opt.*, 2009, **48**(21), 4256-4262. doi: 10.1364/AO.48.004256

ACKNOWLEDGEMENTS

Authors wish to acknowledge Director, IRDE, Dehradun for permitting to publish the work; Head of Photonics Design Centre, IRDE for his encouragement and the members of Adaptive Optics Division for their cooperation. Dr N.S. Vasan is also acknowledged for his guidance. Awakash Dixit is thankful to the DRDO, India for the research fellowship.

CONTRIBUTORS

Dr Awakash Dixit obtained his MSc (Electronics) from UIET, CSJM University, Kanpur, India and PhD (Physics) from DRDO-Instruments Research & Development Establishment/Uttarakhand Technical University, Dehradun, India. He worked as a Senior Research Fellow in IRDE, Dehradun, India. Currently, he is working as a Senior Scientist in Indian Institute of Technology Madras, Chennai, India. His areas of interest are singular optics, atmospheric turbulence, adaptive optics, lithography, micro-optics: Design fabrication and characterisation, and beam combining.

Contribution in current study, he was responsible for conducting the experiment, data recording and data analysis, preparing the manuscript.

Mr Aditya Kumar Mangain obtained his MSc (Physics) from HNB Garhwal University, Srinagar, India. He was working as Scientist in Adaptive Optics Division, DRDO-Instruments Research and Development Establishment, Dehradun. His area of interest include: Adaptive optics and measurements of atmospheric turbulence.

Contribution in current study, he was responsible for conducting the experiment, data recording, data analysis, and preparing the manuscript.

Dr Vikash Porwal received his MSc (Physics) and PhD (Physics) from Lucknow University, Lucknow. He is working as Scientist in Adaptive Optics Division, DRDO-Instruments Research & Development Establishment, Dehradun. His research area includes Adaptive optics, vortex beams, wavefront information processing, etc. He is a fellow member of Optical Society of India, and Indian Science Congress Association.

Contribution in current study, he was responsible for designing the experiment, data interpretation and proof reading.

Dr Sanjay Kumar Mishra received his MSc (Physics) from BHU, Varanasi, MTech (Laser Technology) from IIT-K, Kanpur and PhD in Physics from IIT-D, Delhi. Presently working as Scientist Adaptive Optics Division, DRDO-Instruments Research & Development Establishment, Dehradun. His research area includes : Adaptive optics, vortex beams, wavefront information processing, computer generated holograms, etc.

Contribution in current study, he was responsible for designing the experiment, data interpretation and proof reading.